DEVELOPMENT OF A DEPLOYABLE DECELERATOR CONCEPT FOR SMALL MARS LANDERS

S. Förste[1], *T. Reimer*[2], *I. Sakraker*[2], *L. Witte*[3], *S. Fasoulas*[4]

[1]Student at the DLR Institute of Structures and Design, Space System Integration Department in DLR Stuttgart, Germany
[2]Research Scientist at the DLR Institute of Structures and Design, Space System Integration Department in DLR Stuttgart, Germany
[3]Department Head at the DLR Institute of Space Systems, Landing and Exploration Technologies Department in DLR Bremen, Germany
[4]Head of Institute of Space Systems at the University of Stuttgart, Germany

ABSTRACT

Small exploration spacecraft and landers have proven to be scientifically useful and capable with missions such as Philae or Hayabusa 2. For the exploration of planetary bodies with atmospheres, novel and efficient entry, descent and landing (EDL) technologies are being explored. One of these concepts is the rigid deployable decelerator, which would be an alternative to existing EDL systems if proven to be feasible. For a Mars micro lander mission with an entry mass of $25\,\mathrm{kg}$ and a ballistic coefficient of $3.5\,\mathrm{kg/m^2}$, a concept for a deployable decelerator was developed. First, a flow-field analysis of different possible geometries of the deployed structure with Ansys Fluent was performed. From this, the pressure and temperature distribution and qualitatively the heat flux density along the profile wall of each geometry were determined. Subsequently, for a conical geometry, a design for a deployment mechanism was developed based on the umbrella concept, where a deployable structure spans a flexible thermally resistant cloth. The mechanism developed is a combination of folding parallelised struts, similar to an umbrella, and telescopic rods. Focusing on the strut structure and based on the results of the flow field analysis, with Ansys it was then investigated whether the design can in principle withstand the mechanical loads generated by the maximum dynamic pressure and how the temperature behind the deployed cloth is distributed under the maximum thermal load.

***Index Terms*—** Mars EDL, Deployable Decelerator, Planetary Penetrator

1. INTRODUCTION

The DLR mission scenario envisages a Mars micro lander (MML) probe with a mass of around $25\,\mathrm{kg}$, which will land on the surface of Mars and serve there as carrier for scientific instruments, such as geophysical and meteorological sensors as part of observation networks. The MML consists of the payload and the decelerator system. The payload is carried by a penetrator, which anchors itself in the ground due to its mass and impact speed at touchdown. The aerodynamic decelerator is intended to decelerate the probe in a pure ballistic entry flight from about $6.000\,\mathrm{m/s}$ entry speed to around $40\,\mathrm{m/s}$ at ground impact. The diameter of the projected unfolded braking surface must therefore have a minimum diameter of about $2.4\,\mathrm{m}$. The MML, due to its size, could fly piggyback on a Mars probe as a secondary payload for example, as a replacement for the masses that are thrown off in order to initiate the descent. It is envisaged that the decelerator will deploy after being dropped from the spacecraft before entering the Martian atmosphere as shown in Figure 1. Data from the trajectory, velocity and maximum heat flux density over time for the mission scenario described, are shown in Figure 2.

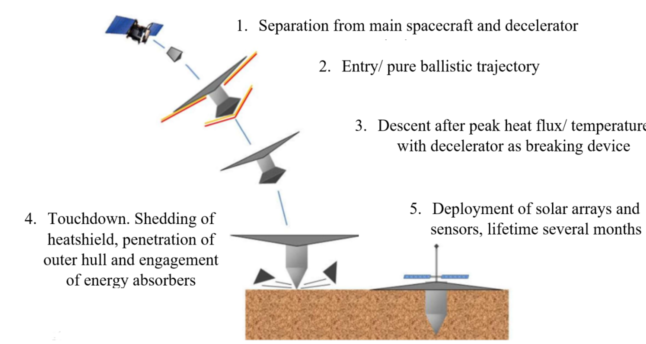

Fig. 1. Mission scenario with possible decelerator design

The conventional architecture for protecting the payload during hyper-velocity entry is a rigid aeroshell, which consists of a thermal protection system bonded to an underlying structure [2]. In order to overcome the limitations of rigid aeroshells for future EDL missions, two new technologies are being developed to realise deployable aeroshells, the inflat-

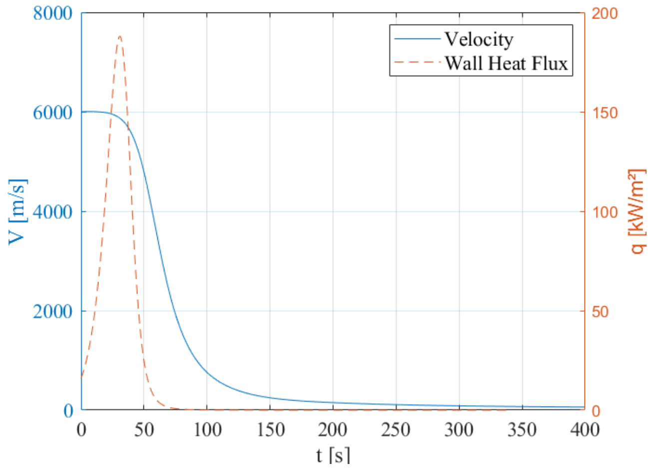

Fig. 2. Trajectory data from DLR MML, velocity over time and maximum wall heat flux density over time. Calculated with a Matlab tool developed by DLR [1]

able aerodynamic decelerator and the rigid deployable decelerator. The MML mission design resembles a similar concept as the Mars MetNet concept proposed by A.-M. Harri [3] where a solution for an inflatable concept was developed.

2. FLOW FIELD ANALYSIS

In general, blunt bodies and large half angle cones provide high aerodynamic drag and low aerothermal heating, which is why they are chosen not only for rigid aeroshells, but also for inflatable solutions although this kind of geometry can show severe aerodynamic instable behavior [4]. Also for most rigid deployable concepts so far, a corresponding geometry is the objective. In this work, flow field analyses in Ansys Fluent with different possible geometries for the MML were carried out to determine the respective aerothermal and aerodynamic loads. For the flow field analysis, only compressible equilibrium flow was considered and therefore no chemical reactions. Therefore results from the flow field analysis carried out with Ansys Fluent in the upper velocity range of the trajectory are not quantitatively reliable. However, since the maximum loads occur in this upper range of fluctuations, i.e. in the hypersonic range, the values from simulations in the supersonic range were scaled with the help of literature values. The maximum heat load at the stagnation point of an entry body is calculated by Fay and Riddell and is $188\,\mathrm{kW/m^2}$. The modified Newtonian theory according to Anderson [5] was used for the determination of the maximum stagnation pressure and is $700\,\mathrm{Pa}$. The initial probe configuration considered a decelerator attached to the rear of the penetrator as seen in Figure 1. This geometry stabilizes the MML on its purely ballistic trajectory in the lower velocity range and the decelerator also does not obstruct the penetrator during impact. This geometry will be referred to as Design 1 in the following. Thermal resistant material such as an ablator at the tip of the penetrator is also provided for this initial design. This geometry and also three alternatives were investigated with respect to their flow fields and occurring loads and are sketched in Figure 3. The meshes for the investigated profiles were iteratively adjusted and optimized with respect to convergence. A structured mesh was always used based on iterative adjustments of the mesh whereby it turned out that for the convergence control of the solution it is easier to use a structured mesh rather than an unstructured mesh. Figure 4 shows the final mesh for Design 4 as an example of this.

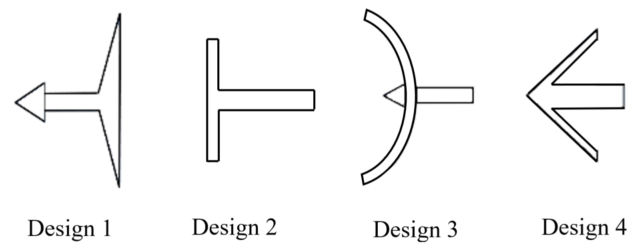

Fig. 3. Four designs for the deployed geometry were investigated with respect to their flow fields.

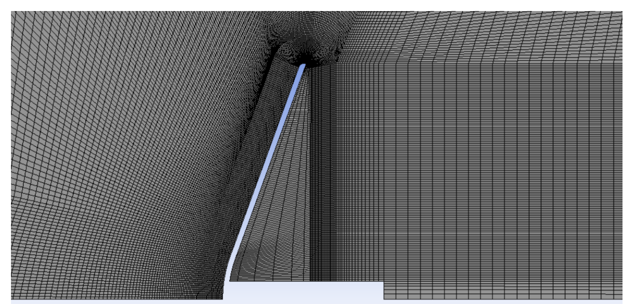

Fig. 4. Example of a structured mesh in Ansys Fluent used for Design 4.

Design 2 corresponds to a geometry that have already been investigated in the context of thermal design of Aeroassisted Orbital Transfer Vehicles (AOTV) and analysed as a reusable, umbrella-like deployable decelerator device for the Space Shuttle [6]. Design 3 is a version of concave hypersonic profiles, some of which have already been studied [7], a geometry that, unlike the other geometries, maximizes heat loads in the outer region of the deployed shield rather than in the nose region. For example, in the SCIROCCO facilies [7], a geometry concave in the stagnation area was investigated for hypersonics. In addition, Design 2 and 3 are geometries that would not be feasible with an inflatable configuration. Design 4 corresponds to the geometry mainly used so far for entry probes, a large half angle cone with an opening angle of 70°. As an example for the flow field analysis solutions, the wall temperature and pressure of the presented geometries are compared in Figures 6 and 5 for an incident flow velocity of $1000\,\mathrm{m/s}$ at an ambient pressure of $8.5\,\mathrm{Pa}$, an ambient temperature of $168\,\mathrm{K}$ and zero AOA. The simulations were carried out with half 2D profiles of the geomertry. The results show the scaled curve of the respective flow magnitude along the 2D profiles starting in the nose area where x is zero and ending at the respective outer edge where x is equal to 1. The magnitude of the temperature or pressure was also scaled over the respective total length along the profile from nose to outer edge.

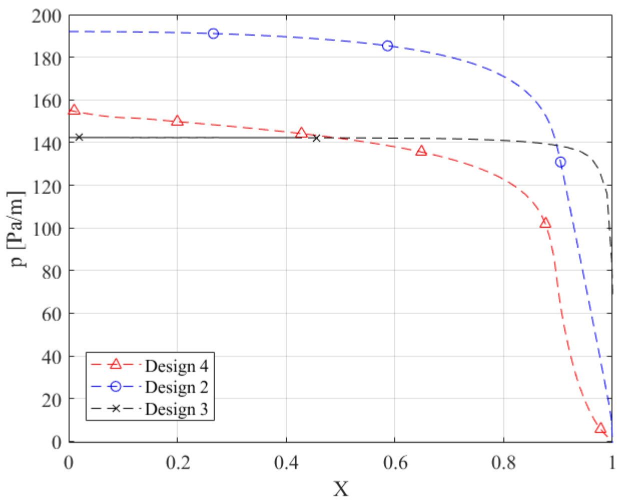

Fig. 5. Static pressure close to the wall of Design 2 to 4 at 1000m/s. The pressure is normalized to the length of the wall along the front of each profile.

The gas mixture properties were taken into account in the inflow conditions by the externally calculated transport properties shown in Table 2. The values were calculated with CEA[1] based on the gas composition in Table 1. The flow field analysis showed qualitative curves for mechanical and thermal loads along the possible geometries.

Table 1. Mars atmosphere composition taken from [8]

Gas	Proportion
Carbon dioxide (CO_2)	95.3 %
Nitrogen (N_2)	2.7 %
Argon (Ar)	1.6 %
Oxygen (O_2)	0.13 %
Carbon monoxide (CO)	0.07 %

The loads for Designs 2, 3 and 4 are in similar ranges. The surface area of Design 3 is larger and accordingly the loads are slightly lower than those for Designs 2 and 4. As no

[1] https://cearun.grc.nasa.gov/

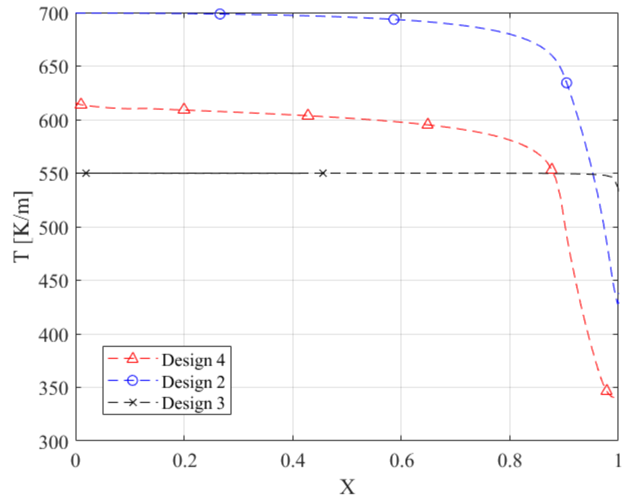

Fig. 6. Static wall temperature of Design 2 to 4 at 1000m/s. The temperature is normalized to the length of the wall along the front of each profile.

Table 2. Mars atmosphere transport properties, calculated with CEA

Parameter	Value
Specific Heat	$700\,\mathrm{J/kgK}$
Thermal Conductivity	$0.0096\,\mathrm{W/mK}$
Viscosity	$1.37 \times 10^{-5}\,\mathrm{kg/ms}$
Molecular Weight	$44\,\mathrm{kg/kmol}$

reliable hypersonic flow field analyses could be carried out due to the simulation framework conditions, it cannot be conclusively assessed whether Design 3 offers a worthwhile advantage in terms of loads. However, there is insufficient data on such a profile so that statements about the flight behaviour and flight stability require a separate investigation. To take advantage of a low ballistic coefficient, the maximum effective diameter should be present before the entry. With Design 3, the tip heat flux loads can be shifted away from the tip towards the outside, but a major hurdle in the design of such a geometry is the aerodynamic stability and the lack of data on the hypersonic area. Also, there is a strongly increased heat flux density at the outer edge, whose absolute amount in the hypersonic region cannot be determined with the present models. For the DLR MML, therefore, a geometry corresponding to Design 4 is being sought. In developing a concept for the deployment mechanism for the DLR MML, the objective is to deploy the support structure for the carbon cloth from the smallest possible storage volume to the target geometry since the lander may be carried as a secondary payload, a single lander or multiple landers at the same time. Deployable decelerators fundamentally pursue the goal of compensating for volume constraints. This means that the area that is to provide the necessary aerodynamic drag during the entry flight must be stored in some form of reduced size. In previous deployable decelerator concepts, this usually means reducing the effective transverse diameter. In the present case, a reduction in the longitudinal extent of the folded decelerator is also considered. The aim of the design is to ensure that the structural parts of the decelerator do not exceed the length of the penetrator in the folded state.

3. DESIGN APPROACHES

Based on the design requirements the following two aspects play a fundamental role in the choice of the design approach for the deployment mechanism:

Aspect 1: Weight and Storage Requirements

With an intended mass of 10 kg for the deployable decelerator, which represents 40% of the total mass of the lander, the decelerator design solution must be extremely lightweight. Furthermore, if the penetrator is to act as a secondary payload, the storage volume might be relatively limited. The unique capability of concepts like ADEPT for small science payloads comes from its ability to stow within a slender volume and deploy passively to achieve a mass-efficient drag surface with a high heat rate capability [9]. It is therefore to be investigated whether a similar design approach can be used for the DLR MML.

Aspect 2: Folded to Unfolded Diameter

Concepts such as Nano ADEPT or the Mechanically Deployable Aero-Decelerator for Mars Entry investigated at the Imperial College London[10] are based on the deployment of a flexible TPS overstretched strut arms. The unfolding principle is similar to that of an umbrella, in which the angle of the struts to each other is changed by displacement at the central joint and the effective aerodynamic drag surface is increased. The required diameter of the MML deployed decelerator is significantly larger in relation to the main body (the penetrator) length, meaning that the deploying main struts have to be artificially extended (e.g. telescope poles mechanism IRENE [11]). Besides the deployment of ribs and struts similar to the ADEPT concept, there are also other conceivable deployment concepts for the use of a flexible TPS. There are considerations for the use of mechanisms of ring and frustum type, cloths that are held open by rotation due to their inertia, or other origami-based folding concepts. These concepts should not be ruled out in principle for use in a micro lander, but a deployable rib-strut structure should serve as the basis for the MML, since there is considerably more data and experience for its use than for the other concepts mentioned. Approaches that reduce velocity by conversion to rotational energy rather than effective drag area were also initially rejected for the DLR MML design because, in order to reduce the area significantly, high frequencies would be required for the present entry conditions, which increase the necessary structural mass.

4. DEPLOYABLE STRUTS

The target geometry for the deployment mechanism corresponds to Design 4 from the flow field analysis. The umbrella principle as in ADEPT is particularly well suited for small scientific payloads due to the achievable slim stowage volume, the possible use of a passive deployment mechanism and a mass efficient drag surface. Therefore, a principle similar to that of an umbrella is chosen as the design approach for the MML deployment mechanism. Since the entire structure is a hot structure, i.e. almost all structural components must withstand temperatures similar to those of the TPS Cloth in the most extreme case, the choice of materials is limited in this respect. Materials that meet these requirements, are generally not suitable for the manufacture of springs or particularly flexible components. Mechanisms with parallelised struts are used in umbrellas. In these, thin metallic struts and additional flexible elements made of metal are used to create an even surface in the stretched textile. This flexibility in the structure allows tension to be created in the unfolded textile. Pretensioning is required in the TPS fabric to provide the necessary stability. The pre-tension is generated when the decelerator is in the unfolded state. The decelerator is then folded, giving the spring its potential force, and the central ring is fixed to a hold down and release device. Thus folded, the MML is launched. Since metallic materials along the struts should be avoided for the DLR MML, in order to create an effect similar to that of umbrellas, the struts, which could be made of carbon fibre reinforced carbon (C/C) or carbon fiber-reinforced silicon carbide (C/C-SiC), for example, could be chosen to be correspondingly thin. The structure would accordingly be very flexible during entry. This aspect has already been partially investigated for entry probes [12]. Flexible structures can have a significant impact on the entry trajectory, but the predictability of the loads can become extremely complex. If a high degree of flexibility in the struts is to be avoided when using the umbrella principle, the quasi-rigid struts must be arranged in such a way that they still create the necessary tension in the textile when unfolded. The umbrella principle could not be directly transferred to the MML because the maximum strut length is limited by the maximum length of the payload volume. The mechanism was therefore extended by an additional mechanism. Attempts to compensate for this limitation with additional joints and struts result in a higher number of rotating joints, which can be detrimental to the predictability and reliable operation of the mechanism, and more complicated folds and structural connection options of the TPS fabric. Some concepts as presented in the context of IRENE [11] envisage the use of telescopic poles as an alternative solution to concepts like ADEPT. With telescopic poles, a very small storage volume can be achieved with a simultaneously smaller number of rotary connections, but the opening process is complex. Figure 7 shows a combination of parallelized struts and a telescope mechanism for the extension of the main struts.

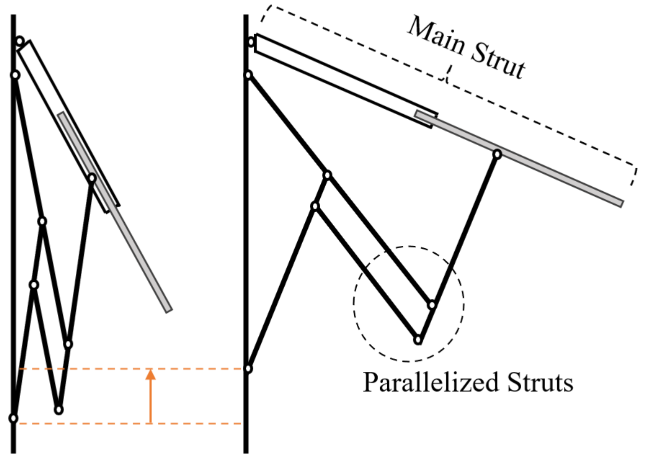

Fig. 7. Combination of an umbrella mechanism with telescopic main struts

This design solution allows the use of quasi-rigid struts. An important design parameter for concepts of this type is the number of arms. The number influences the convexity of the folded TPS cloth. This in turn has an influence on the actual heat and pressure load distribution on the windward side of the cloth. In addition, the number of arms affects the flexibility of the unfolded structure, since a higher number of arms requires a reduction in the material thickness of the struts while the total mass remains the same. The number of arms is initially set at eight. The more arms used, the less pronounced the corners created in the stretched cloth. This mechanism is very easily adaptable with regard to the deployed opening angle and could also be used for a geometry corresponding to Design 2. The number of arms is initially set to eight in order to be able to create a rather higher stiffness in the struts.

The flexible TPS is stretched by the main struts. The cloth geometry has a hole in the middle in the nose area. This is where the maximum heat loads occur, which is why ablative material is used as a cap in the nose area as shown in Figure 9. The design principle for the DLR MML is that the entire decelerator is a hot structure. Accordingly, the material for the structural elements must withstand high temperatures as well as mechanical loads. Materials with ceramic components are suitable for such requirements. Since the actual thermal and mechanical load response is yet to be determined, C/CSi-C [13] is chosen for the structure, mechanical connections and bearings. This fiber-reinforced ceramic can withstand temperatures of up to about 1600°C [14] and at the same time has a sufficiently high mechanical load-bearing capacity.

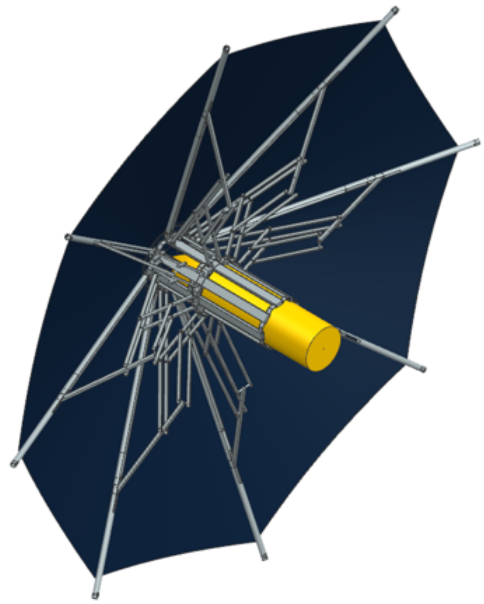

Fig. 8. Isometric view of the final design in a eight-arm version, unfolded decelerator with unfolded TPS fabric, central structure and penetrator cone

5. DEPLOYMENT ACTUATOR

The Decelerator is passively opened in a single stage. Opening is accomplished by means of preloaded springs and the process is initiated by a simple hold down and release mechanism commonly used in space mechanisms. The design and layout of the hold down and release mechanism is not part of the considerations made here. The arms are all connected via a central ring, so the opening driver can theoretically be positioned at any joint or at the central ring, all arms always unfold. In order for the struts to be folded into each other, some of the arms must be arranged in a double parallel way.

Two different spring configurations are proposed for the opening mechanism, firstly the use of torsion springs, which press the struts open via a torque directly at a joint. When using the torsion spring configuration, the springs are located on the rotatable bearing of the main struts below the ablative cap. The alternative configuration uses tension or compression coil springs that move the central ring directly. The disadvantage of coil spring configuration is the long spring deflection. In the MML design, the spring deflection needed would be $270\,\mathrm{mm}$ for the coil spring configuration. If the springs were positioned in the area of the central ring, the springs might have to be shielded and the volume available for the spring would require the use of serpentine long coil springs. At $270\,\mathrm{mm}$, however, the spring travel is already close to the limit of the maximum spring deflection of coil springs of this configuration. Due to the long space travel phase, such a spring could lose significant pretension. This loss becomes

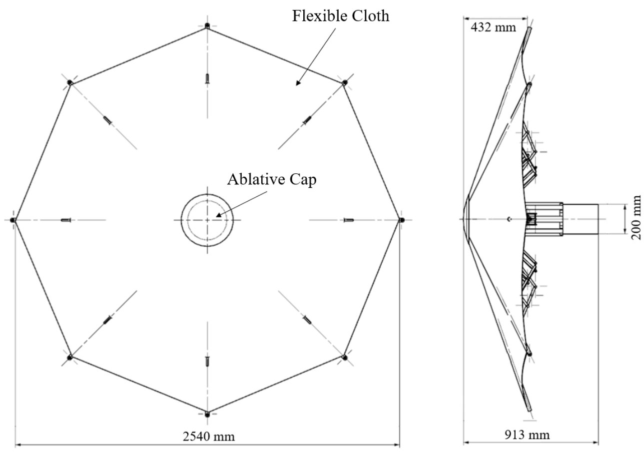

Fig. 9. Technical drawing representation of the DLR MML with decelerator deployed, TPS system and with dimensions.

greater with increasing spring deflection. Another possibility for the design of the spring mechanism would be to use a roller with an integrated pretensioned spring onto which a rope is wound. This would also allow large travels to be realized and would compensate for the problem of long spring travel in the coil spring configuration. Rope hoists are proven in space technology for the deployment of complex structures. Nevertheless, the use of torsion springs avoids the problem of long spring deflection. The torsion spring configuration appears to be the simplest if the necessary torque can be applied to open and tension the screen, and due to the positioning of the torsion springs, they would most likely not require any further shielding, since the temperatures should be among the lowest below the ablative cap. Which spring principle is most suitable can be determined in practical tests.

6. PERFORMANCE ANALYSIS

The occurring maximum dynamic pressure load is used as the dimensioning load for the bolts, bearings and the locking device and for the FEM analysis of the struts. A static analysis using the internal forces method for a single unfolded arm gave first approximate values for the maximum pin load as well as the dimensioning of the springs of both spring concepts of the passive opening mechanism. Planned practical tests with the help of a prototype and feasibility tests during component manufacture in relation to the proposed materials should provide more precise results. With regard to the spring dimensioning, the provision of the necessary tension in the cloth before engagement plays a central role and this must also be investigated in practical trials.

Here, the unfolded struts and the stresses under the maximum compressive load were investigated in more detail with regard to performance. The analysis with Ansys Mechanical approximates the actual pressure curve taken from the flow field Analysis in Ansys Fluent shown in Figure 10.

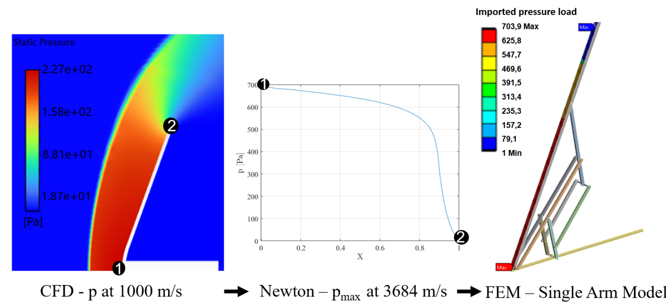

Fig. 10. Principle of load data transfer from flow field analysis for static mechanical FEM load analysis

Figure 11 shows a section of the FEM model in which the maximum principal stress distribution under the maximum compressive load was calculated. Figure 11 shows the maximum load calculated by Ansys occurs in the area of bearing A and is 2.7×10^8 Pa. Due to the long lever arm of the pressure load at bearing A, it can be assumed that bearing A is realistic as the location of higher loads. However, the stress peak only occurs over individual elements and the mesh in the area of the bolts is roughly chosen. Therefore, the stress peaks could be a numerical artefact and the actual stress peaks could be significantly lower.

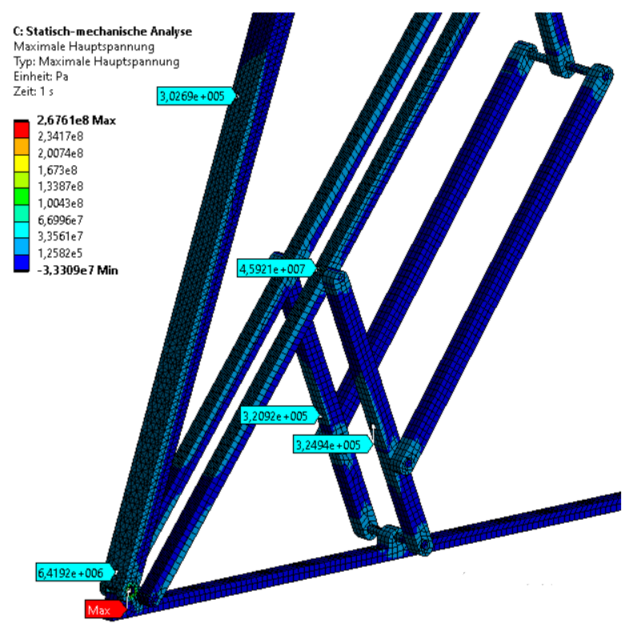

Fig. 11. Maximum principal stress distribution in the struts at maximum compressive load

The actual maximum stressin the struts is 4.5×10^7 Pa. At a maximum bending stress of 4.5×10^7 Pa, the safety factor of the struts made of C/CSiC would be 0.38 for a breaking stress of 120 MPa. However, the stress values in the remaining areas of the structure are in the lower Megapascal range or below 1 MPa. The results show that the struts made of C/CSiC are still oversized and, if necessary, weight could be saved here in a further design iteration step by downsizing the strut thickness or using lighter materials such as carbon.

How much of the heat loads the structure materials must carry highly depends on the radiation from the back shield. The maximum heat flux density for the DLR MML is $188\,\mathrm{kW/m^2}$. To investigate the heat loads at individual significant positions such as structural components and the payload, a thermal steady-state analysis in Ansys was used. Figure 12 shows the temperature distribution along a substitute model with the deployed carbon shield, for which the thermal conductivity was assumed to be $25.7\,\mathrm{W/mK}$, a single deployed structural arm and the payload geometry, the penetrator. The heat flux of $188\,\mathrm{kW/m^2}$ was imprinted on the front of the decelerator surface and all structural components radiate with an emissivity of 0.8 and are in radiation exchange with all geometries and the environment. Heat is now also exchanged between the penetrator and the decelerator via heat conduction across the structure.

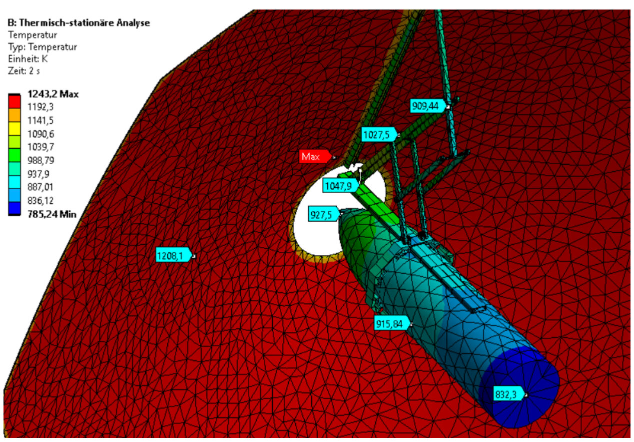

Fig. 12. The maximum temperature at the carbon TPS fabric is 1243 K, the maximum temperature at the struts just under 1050 K and the maximum temperature of the payload just under 930 K.

Since the housing of the penetrator is a metallic structure, thermal protection, for example in the form of an insulating coating, should be considered to protect the payload. The temperature loads on the struts are in the range of a maximum of just over 1000 K. Since the temperature limit for a structural component made of C/CSiC is around 1600°C, i.e. over 1870 K, the temperatures occurring here are therefore not critical for the material and the structural integrity. The alternative use of carbon struts can be considered in view of the calculated temperatures for possible mass savings.

In addition, the qualitative wall heat flux density curve for the deployed decelerator is shown in the Figure 13, calculated with Ansys Fluent.

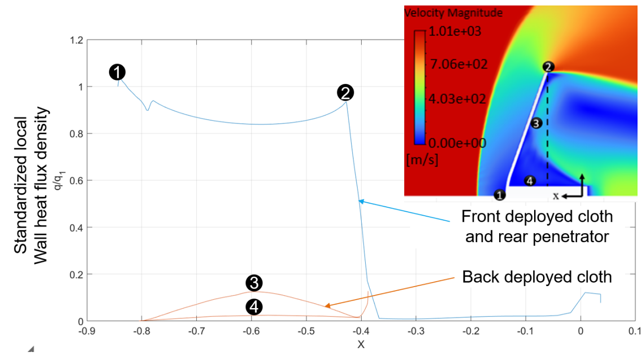

Fig. 13. Wall heat flux density of the deployed decelerator geometry with non-adiabatic wall

7. CONCLUSIONS

For the DLR MML mission, a rigid deployable decelerator concept was developed. For this, four different possible target geometries for the deployment mechanism were considered and their flow fields analysed with Ansys Fluent. Based on this, a target geometry for the deployed decelerator was chosen, a geometry corresponding to the conventional half angle cone, and a design for the deployment mechanism was developed. For the DLR MML, a design solution based on the umbrella principle was developed. For the DLR MML, this principle was extended by a combination with telescopic poles in order to achieve the necessary surface with the smallest possible number of struts and joints. The structure unfolds with the help of a passive mechanism via pre-tensioned springs, for which two spring configurations were investigated. With focus on the strut structure, a load analysis of mechanical and thermal loads, which were determined with the flow filed analysis in Ansys Fluent, was carried out to estimate whether this design can withstand the loads during entry and is therefore suitable. Using Ansys, a static load analysis of parts of the unfolded structure was performed on a substitute model using the finite element method. Using this method, a thermal analysis was also carried out to determine how the temperature behind the decelerator is distributed due to combined thermal conduction and radiation and to estimate what temperatures are reached in the payload region.

The flow field analysis of the MML geometry could be performed only limited to the supersonic region. The influence of flow and chemical reactions in the hypersonic region should be investigated in the further course of development. Furthermore, the feasibility of the mechanism principle must be verified with the help of an appropriate prototype. The flexibility and the associated folding possibilities and the structural interface of the TPS fabric to the unfoldable structure represent further core aspects of subsequent development steps. The mechanical analysis also showed that the design can theoretically withstand the loads and that the dimension of the struts can be corrected downward to optimize the structural mass ratio. Also the optimal dimensioning of parts such as the ablative cap and the TPS cloth are tasks for further development as well as finding an optimum for the number of arms. The previous design has shown that with the materials used so far, the mass limit might be difficult to keep and it is recommended to consider the use of other, possibly ceramic-free materials such as carbon for the structural components in order to save weight. Impact also plays a critical role in the design of the MML decelerator, and further development will need to explore how to extend the mechanism so that the deployed decelerator does not impede impact. The construction of a prototype and the first practical tests in a simplified plasma wind tunnel are planned as a continuation of this thesis, as well as the more detailed FEM analysis of the bolt connections and the further optimization of the design. In addition, the next design step deals with the practical implementation of the TPS interface to the structure.

References

[1] A. Schneider, *Numerische Untersuchung der Abstiegs- und Landetrajektorie eines Mars-Mikrolandesystems*, Masterarbeit, Universität Bremen [elib.dlr.de/106323], 2016.

[2] E. Venkatapathy, R. Beck, D. Ellerby, J. Feldman, P. Gage, M. Munk, and P. Wercinski, *Development Challenges of Game-Changing Entry System Technologies From Concept to Mission Infusion*, IEEE, 2016.

[3] A. Harri, K. Pichkadze, L. Zeleny, L. Vazquez, W. Schmidt, S. Alexashkin, and O. Korablev, "The metnet vehicle: a lander to deploy environmental stations for local and global investigations of mars," Feb 2017, IAC 2020 -71st International Astronautical Congress.

[4] G. Herdrich, *Atmospheric Entry Technologie - Introduction*, Lecture Slides Atmospheric Entry Technologie 2020/21 (Uni Stuttgart,IRS).

[5] J. Anderson, *Modern Compressible Flow*, McGraw-Hill, 1990.

[6] Edited by H. Nelson, *Thermal Design of Aeroassisted Orbital Transfer Vehicles*, American Institute of Aeronautics and Astronautics,, 1985.

[7] B. Capra, J. Moran, M. Brown, and R. Boyce, *Aerothermal Analysis of 3D Concave Cone in Hypersonic Flow in SCIROCCO*, 32nd International Symposium on Shock Waves, Jul. 2019.

[8] J. Baumgart, T. Magin, P. Rini, G. Degrez, and O. Chazot, *Simulation of Entry in the True Martian Atmosphere*, Proceedings of the Fifth European Symposium on Aerothermodynamics for Space Vehicles, November 2004.

[9] B. Smith, A. Cassell, and E. Venkatapathy, *ADEPT for Secondary Payloads*, NTRS, 2019.

[10] L. Peacocke, D. O'Driscoll, P. Bruce, and M. Santer, *Mechanically Deployable Aero-Decelerator for Mars Entry*, International Conference on Flight Vehicles, Aerothermodynamics and Re-entry Missions and Engineering (FAR 2019), Sep. 2019.

[11] R. Savio, R. Aurigemma, and P. Dell'Aversana, *European Sounding Rocket Experiment On Hypersonic Deployable Re-Entry Demonstrators*, 8th European Symposium on Aerothermodynamics for Space Vehicles, March 2015.

[12] L. Peacocke, P. Bruce, and M. Santer, *Coupled Aerostructural Modeling of Deployable Aerodecelerators for Mars Entry*, Journal of Spacecraft and Rockets, March 2019.

[13] Edited by N. Bansal, *Handbook of Ceramic Composites*, Kluwer Academic Publishers, 2005.

[14] W. Krenkel, *Carbon Fibre Reinforced Silicon Carbide Composites (C/SiC, C/C-SiC). In: Bansal, N.P. (eds) Handbook of Ceramic Composites.*, Springer, Boston, MA, 2005.